IRAQI JOURNAL OF APPLIED PHYSICS
Vol. 22, No. 4, October-December 2026, pp. 562-568

Aya N. Abdullah [1]
Tahseen A. Aswad [2]
Moaz M. Shukr [3a,b]
Salih Y. Darweesh [4*]

[1] Physics Department, College of Education for Pure Science, Kirkuk University, Kirkuk, IRAQ
[2] The Directorate General of Education in Salah AL-Deen, Salah Al-Deen Province, IRAQ
[3a] Physics Department, College of Imam University, Tikrit, IRAQ
[3b] The Directorate General of Education in Salah AL-Deen, Salah Al-Deen Province, IRAQ
[4*] Physics Department, College of Science, Tikrit University, Tikrıt, IRAQ

Surface Enhancement of Turbine Blades Using Al_{50}-Ni_{50}/TiO_2 Composite Coatings

A base of $Al_{50\%}$-$Ni_{50\%}$ metal was reinforced using TiO_2 with different weight percentages of 5, 10, 15, 20 and 25 wt.%. A flame thermal spray device was used to prepare samples those were sintered at 1000°C for 90 min. It was found that the best mixing ratio was 20 wt.%. After thermal sintering, the results of the SEM showed a mesh and crystalline consistency at this ratio, which shows that all properties were improved at that ratio, while the microhardness at the same ratio was 693 kg/mm^2. It was found that the minimum sliding wear is 1.01×10^{-7} g/cm, while the results of thermal tests revealed that the best mixing ratio is 25 wt.%. Following thermal sintering, it gave thermal conductivity of 125.43 W/m.K, heat capacity of 713.881 J/kg.K, thermal diffusion of 0.424 mm^2/s, thermal flow of 701.711 W.S$^{1/2}$/m^2.K and thermal resistance of 0.0543 m^2.K/W.

Keywords: Thermal resistance; Coatings; Hardness; Flame thermal spray

1. Introduction

Many turbine blades and devices exposed to high temperatures suffer from rust and external corrosion of their surfaces [1]. This phenomenon, which distorts the external surface and reduces the performance of the product, must be addressed [2]. The surface treatment methods vary, from the form of a very simple cover representing the pigments to a metal-ceramic coating characterised by high hardness and wear strength, in addition to strengthening the product [3]. Among the many devices that suffer from thermal corrosion are turbine blades that can be used in electric power plants, industrial engines, submarines and aircraft engines [4]. External thermal corrosion of the blade reduces performance and fuel consumption, and thus, replacing those turbine blades is extremely expensive [5]. Thus, this external wear is treated in several ways, including thermal spraying, which acts as a protective cover, the thickness of which ranges from a few micrometres to a few millimetres [6].

Thermal spraying with a flame is a common method for treating external surfaces and covering them with various materials that contribute to preventing rust or external corrosion [7]. The thermal flame spraying method is divided into many types, including high-speed ox fuel spraying, explosive spraying, wire spraying, electric arc spraying, plasma spraying and thermal flame spraying. Because of the simple cost and the availability of two bottles of oxygen and acetylene, in addition to the resulting samples suitable for the work, the thermal spray method with a flame is typically used [8,9]. This method can be used at room temperature and without the restrictions of the vacuum environment [10]. It is also possible to use a protective coating that contributes to protecting the surface and resolving the problem of thermal corrosion, thus prolonging the product's operation and practical life [11]. This method also improves the mechanical properties of hardness, adhesion strength and sliding wear, which increases the strength of the product and helps it withstand high pressures and friction [12]. Hence, it is possible to obtain economic feasibility when dealing with thermal flame spraying, reducing the high cost, which contributes to the repair of damaged parts [13]. Through this technology, the thickness of the coating can also be controlled with high precision to ensure suitability for the required application [14].

A wide range of material powders can be used in the thermal flame spraying technique, starting with metals such as aluminium, nickel and chromium. These metals improve the properties of the product, strengthen it and increase its hardness [15]. In addition to titanium, nickel and cobalt alloys, there are several materials that effectively shield surfaces operating in harsh environments. These materials include ceramic and porcelain substances such as titanium oxide (TiO_2), aluminium (Al) oxide, silicon oxide and other carbides [16]. There is, thus, a wide range of materials that can be used to serve as an excellent protective coating for turbine blade surfaces [17]. It is possible to use a metal-based mixture of materials supported by ceramic, or vice versa, to give a strong product known as cermet materials (ceramic-metal) [18]. These materials exhibit high levels of hardness, durability and wear resistance, as well as exceptional thermal properties that can be applied to minimise heat transfer to internal components [19,20].

This article aims to study the effect of the thickness of the coating, the type of heat treatment and the coating distance on the structural, mechanical and thermal properties of a metal-based cermet alloy of aluminium–nickel reinforced with ceramic of TiO_2 at different ratios. The goal is to determine the most important results that contribute to solving the problems suffered by plaguing materials.

2. Materials and Methods

Nickel (Ni) and Al powder (Sulzer Metco, Wohlen, Switzerland) were used as base materials with a particle size of <75 µm and a purity of 99.5%. The reinforcement materials were TiO_2 (Shanghai Zhiyuan Powder Material Co., Ltd, China), with a particle size ≤100 µm and a purity of 99.9%.

The flame thermal coating method (GH-4/h, China) was used, mainly using two bottles of oxygen and acetylene, where the pressure ratio for acetylene and oxygen was 0.7 bar and 4 bar, respectively. A schematic of the device is presented in Fig. (1).

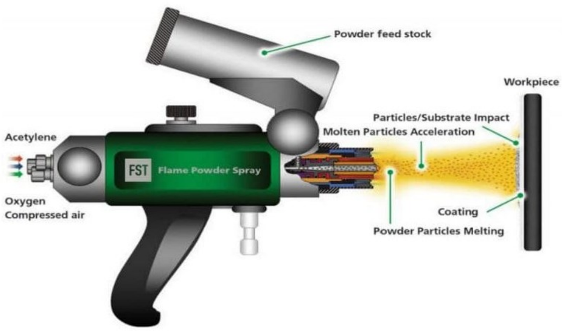

Fig. (1) Flame spray technology device

The paint distance between the base and the coating gun was fixed at 16 cm, with a paint angle of 90°. The base was made of out-of-service turbine blades that were cut to a diameter of 20 mm and a height of 5 mm to fit on the stand for the prepared bases. The base was roughened using a serration method to increase the adhesion of the molten materials in droplets to the surface. Powders were mixed from the base material (Al_{50}–Ni_{50}) in equal proportions and reinforced with a binder of TiO_2, with reinforcement ratios of 5, 10, 15, 20, and 25 wt.%. The two powders were mixed and ground in a homemade grinder and dried in a convection oven at 100°C. The powders were placed after dividing the specified proportions into the device's pod, and the device began to operate gradually, starting with acetylene, then oxygen, before opening the powder tap to force it at high pressure into the main nozzle such that the liquid droplets rush to the surface of the sample bases. The prepared samples were left to cool and then inserted into a thermal oven for sintering. A Korean-origin Muffle-type oven (MF-12, serial number: HYO170382) was used at 1,000°C for 90 min. After turning off the oven, the samples were left until the next morning to settle further. The samples removed from the convection oven were smoothed with 2000-grit silicon carbide paper, after which they were ready for the structural, mechanical and thermal tests.

Structural examinations were performed using scanning electron microscopy (SEM) and X-ray spectroscopy (EDS). The microscope is a tool used to examine the surface topography of paint to identify any external structures with high precision. This allows for the identification of surface defects such as pores, cracks and surface dislocations, which can greatly affect the physical properties of the paint. After detecting these defects, they can be treated accordingly, resulting in an improved final product [21]. Using SEM, it is also possible to measure the thickness of the coating, which provides the quality of the resulting samples and how to improve them. It is also possible, through EDS, to determine the elemental composition of the resulting alloys and their chemical composition, as well as the types of materials included in the alloys. In general, the SEM method plays a crucial role in the analysis and characterisation of thermal flame spray coatings [22].

The Vickers-type microhardness test was conducted using a French-made METKON hardness device. This device consists of a penetration tool that has a tapered microscopic head in the shape of a square diamond pyramid. The planes of the pyramid intersect at the top at an angle of 136°. The sample for the test is fixed under this tool. It applies a load of 50 N in a time of 20 s. The Vickers hardness number is calculated by measuring the lengths of the two diagonals (d_2, d_1) and their average value (D) and then applying the relationship [18,23], as follows:

$$HV = 1.854\ \frac{P}{d_{av}} \quad (1)$$

where HV is Vickers hardness, P is applied load (Kg) and d_{av} is average impact diameter (mm^2).

The sliding wear test was performed using the (Disc method), where the samples were weighed after removing them from the oven to represent the initial weight w_1. Following this, the sample was placed in the jaw of the device, which applied a constant load of 25 N and a constant rotational speed of the disk at 400 rpm for 15 min. The device was then stopped and the sample weighted to represent the final weight w_2. The wear rate was calculated using the relationships below [19,24]:

$$wear\ rate = \frac{m_1 - m_2}{d} \quad (2)$$

where m_1 is weight of samples before the test, m_2 is weight of samples after the test and d is the distance travelled during the test, which can be found using the following equation [24]:

$$d = 2\pi RN \quad (3)$$

where R is the radius of the samples used and N is the number of cycles of the wear device.

The thermal properties of the coated samples were calculated following thermal sintering to determine the ability of the samples to conduct thermally. These coatings are used as heat insulators because heat has a significant effect on the coating layers. The device used to measure the thermal conductivity was the Mathis TCi type (MPTS). The device is based on the principle of thermal analysis to measure all thermal variables. The thermal conductivity and heat flow are measured directly, giving a detailed presentation of the thermal properties of the sample materials, which may be in the form of solid, liquid, powder or pasty material [25,26]. The remainder of the thermal properties can be calculated using mathematical relationships.

The thermal conductivity was calculated using the following equations [26–28]:

$$Q = \frac{\mathrm{dH}}{\mathrm{dt}} = -\frac{\lambda A\, dT}{dx} \quad (4)$$

where Q is the amount of heat per unit time (W), H is heat (J), t is time (s), λ is thermal conductivity (W/m.K) and T is temperature (K),

$$\delta = \frac{\lambda}{\mathrm{Cp}\,.\rho} \quad (5)$$

where Cp is specific heat capacity (J/g.k) and ρ is sample density (g/cm^3).

The thermal Effusion relationship Ɛ (Ws½/m^2. K) is:

$$\varepsilon = \sqrt{\lambda\,.\,\rho\,.\,\mathrm{Cp}} \quad (6)$$

The thermal resistance $R_{thermal}$ (m^2.K/W) is:

$$R.thermal = \frac{\mathrm{dX}}{\lambda} \quad (7)$$

3. Results and Discussion

The results obtained from structural tests using SEM and EDS were analysed following heat treatment of the samples that were coated at different concentrations, as shown in Fig. (2), at 5kX magnification and a depth of 10 µm. As the figure shows, the reinforcement ratios had a random and irregular surface, and they also contained a number of cracks and pores that weakened the paint. However, at high reinforcement (Figure 2d, e), the pattern was more regular and intertwined between the paint elements, while there was also more homogeneity and a more crystalline arrangement than other shapes. As the metal base material contributes effectively at high temperatures to bonding the paint with the ceramic support material of TiO_2, the sintering temperature of 1000°C contributes significantly to the integration of the coated grains. We also found that the high flame temperatures of the thermal spray gun affected the condensation of the crystalline structure, which, in turn, increased the hardness and durability of the painted models, and the fusion that occurred between the metal and ceramic led to interfacial interactions that contribute to strengthening the resulting alloy [19,29]. Consequently, surface and interfacial cohesion of the elements was achieved, with a significant improvement in thermal and mechanical performance. The effect of adding the TiO_2 reinforcement material had a significant impact on the crystalline structure in terms of changing the shape and size of the crystalline grains in the coating, which led to a granular distribution that resulted in a reinforcement ratio of 25wt.%. There was also a chemical change that led to enhanced bonding between the grains of all the coated elements. Thus, increasing the percentage of ceramic material contributed to improving the structural properties of the models painted using the thermal flame spray method and enhanced the ability of these coatings to resist heat, corrosion and bending [30,31].

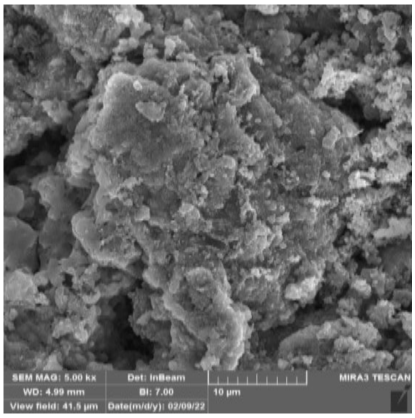

(a)

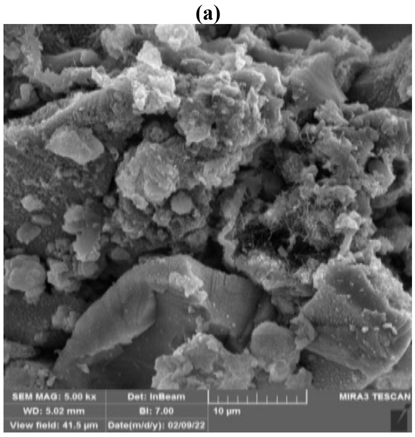

(b)

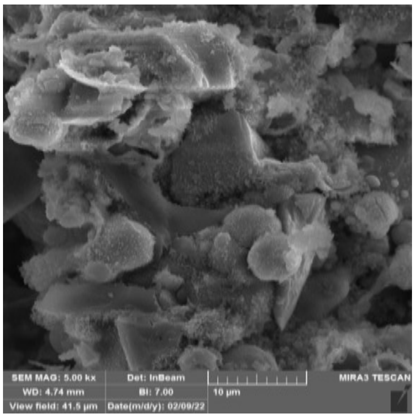

(c)

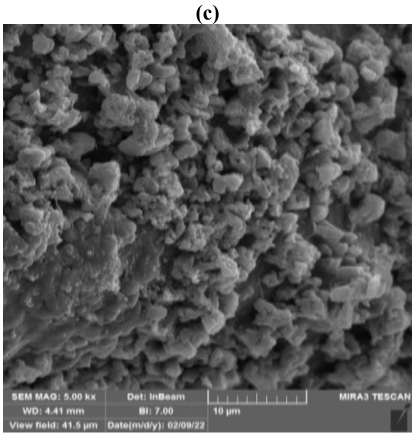

(d)

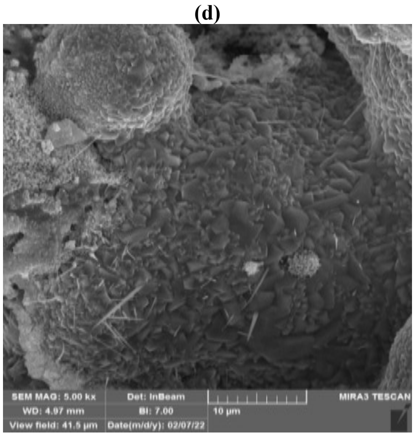

(e)

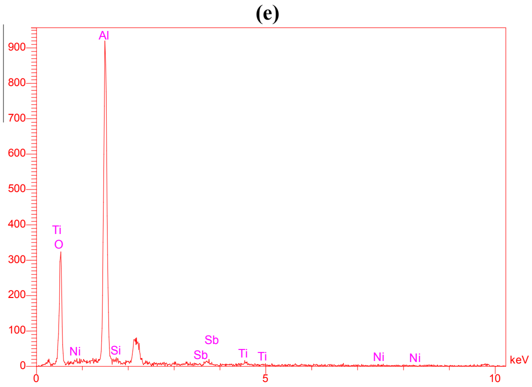

(f)

Fig. (2) SEM images at different reinforcement ratios of TiO_2 after thermal sintering (a) 5 wt.%, (b) 10 wt.%, (c) 15 wt.%, (d) 20 wt.%, (e) 25 wt.%, and (f) EDS spectrum

Figure (3) shows the relationship between Vickers microhardness and TiO_2 reinforcement ratios before and after thermal sintering. Here, it was found that the Vickers hardness before sintering ranged from 402 to 483 kg/mm^2, with a reinforcement ratio of 5-25 wt.% before thermal sintering, while the hardness ranged from 564 to 670 kg/mm^2, with a reinforcement ratio of 5-25 wt.% after thermal sintering at 1000°C. At the same time, the hardness values improved at the best percentage of 20 wt.% to reach 693 kg/mm^2 following thermal sintering. Thus, the addition of TiO_2 greatly strengthened the cermet alloy, but by increasing the high reinforcement ratios by more than 20%, the hardness decreased; this can be attributed to the accumulation occurring between the crystal boundaries, which acts as an obstacle to the bonding process between the elements, thus leaving gaps and pores that weaken the cermet coating [32]. In addition, the condensation of oxide-supported materials will overwhelm the proportions of existing metals and thus cause dislocations that weaken the hardness and durability. High temperatures also cause an increase in hardness because heat leads to the condensation of the crystalline structure and the proximity of the grains to each other, thus forming a strong cermet alloy [33].

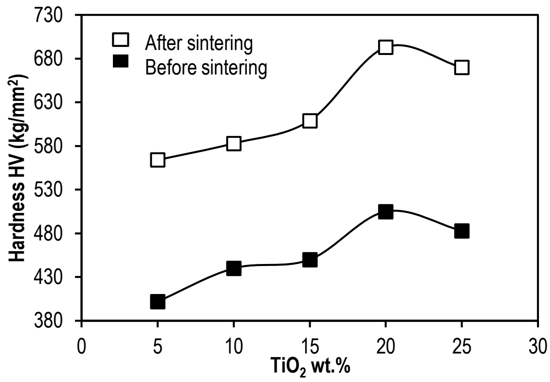

Fig. (3) The relationship between Vickers hardness and TiO_2 reinforcement ratios after thermal sintering

Figure (4) shows the relationship between the rate of sliding wear and the reinforcement ratios added from TiO_2 before and after thermal sintering, respectively. Here, the wear rate at 5 wt.% before sintering was $1.92x10^{-4}$g/cm, whereas after sintering it was $1.59x10^{-6}$g/cm. By increasing the reinforcement ratios, we obtained a wear rate of 20 wt.% before sintering at $1.40x10^{-5}$g/cm, whereas after sintering, it was 1.01×10^{-7}g/cm; the wear rate then increased at rates higher than 20wt.%. The low wear rate can be attributed to the fact that the addition of TiO_2 contributes to strengthening the metal because the oxides have a high resistance to corrosion.

The interaction of TiO_2 with nickel and aluminium works to form a protective layer on the surface of the outer coating that acts as a protective barrier against external influences. In addition, this interaction

IRAQI JOURNAL OF APPLIED PHYSICS
Vol. 22, No. 4, October-December 2026, pp. 562-568

contributes to a high adhesion force that reduces the possibility of the paint breaking or cracking and thus contributes to reducing the wear rate [34]. In general, oxides also reduce chemical corrosion, meaning TiO_2 contributes to reducing chemical reactions and, therefore, limits the rate of sliding wear. Thermal sintering also improves the properties of the painted models and their resistance to corrosion, thus prolonging the life of the paint layer [35].

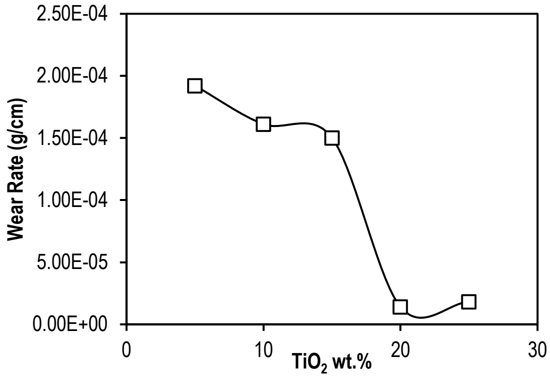

(a) Before sintering

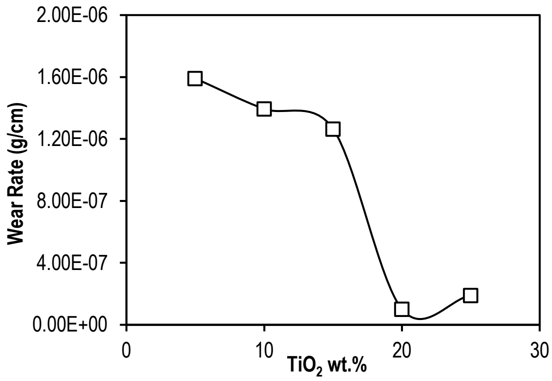

(b) After sintering

Fig. (4) The relationship between wear rate and TiO_2 reinforcement ratios (a) before and (b) after sintering

Figures (5-9) show the relationship between thermal conductivity, heat capacity, thermal diffusion, heat flow and thermal resistance, respectively, with the reinforcement ratios added from TiO_2 after thermal sintering at 1,000°C. Here, adding TiO_2 to the metal base material led to a decrease in thermal conductivity, and this is what is expected of the final results of the resulting coatings. The resulting coating must have low thermal conductivity to ensure that high temperatures do not reach the base of the turbine blade, and it was found that the oxide contributed effectively in this respect, with the same result obtained with the rest of the thermal variables [36,37]. The TiO_2 particles spread across the surface of the metal base material, which led to a change in the crystalline structure and thus affected the distribution and transfer of heat through the coated samples. Furthermore, TiO_2 also has the advantage of thermal storage, thus reducing the arrival of heat to the main surface of the turbine blade, forming a protective layer that reduces thermal conductivity and thermal diffusion and increasing thermal resistance. The best thermal resistance was achieved with a ratio of 25 wt.% TiO_2 at 0.0543 w/m^2.K. Thus, the reinforcement material significantly contributed to reducing thermal conductivity, which is the case with all oxides, preventing heat from reaching the surfaces of the paint bases [38,39].

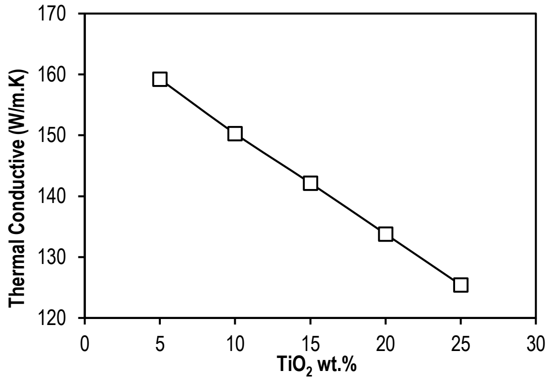

Fig. (5) The relationship of thermal conductivity with reinforcement ratio

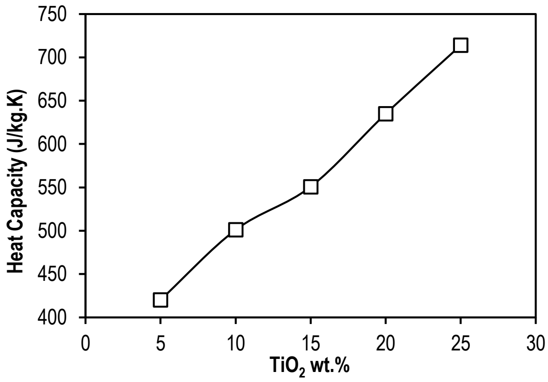

Fig. (6) The relationship of heat capacity with reinforcement ratios

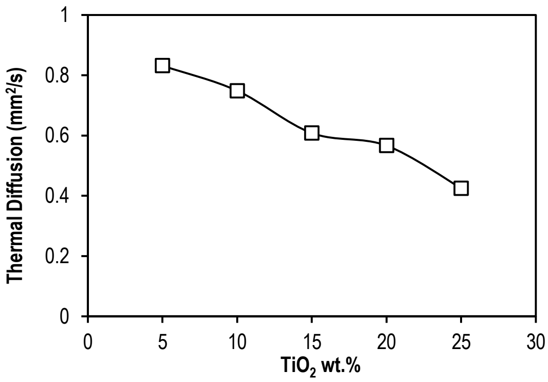

Fig. (7) The relationship of thermal diffusion with reinforcement ratios

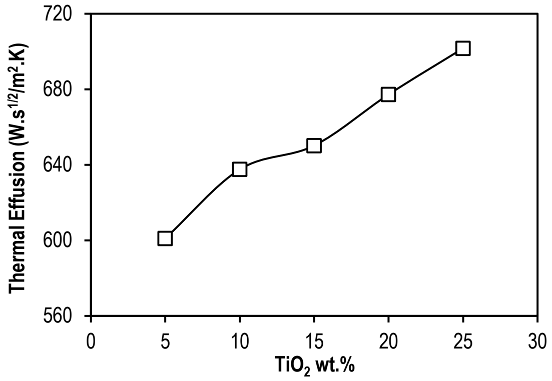

Fig. (8) The relationship between thermal effusion with reinforcement ratios

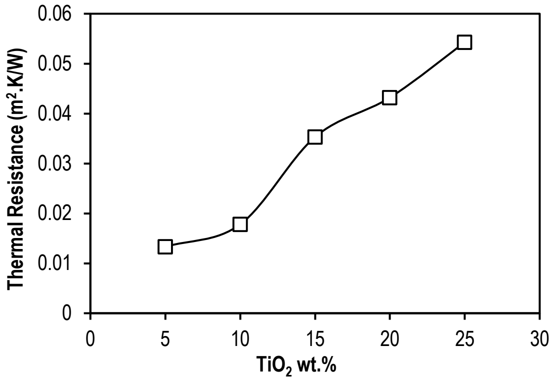

Fig. (9) The relationship between thermal resistance with reinforcement ratios

4. Conclusion

This study found that adding TiO_2 to the base material of Al_{50}–Ni_{50} has a significant impact on the formation of an alloy with distinct physical properties. It was found that the best mixing ratio was 25wt.% for the structural and thermal properties, whereas the best mixing ratio for the mechanical properties was 20wt.%. Encouraging structural properties were also obtained in terms of the regularity of the crystal structure and mechanical interlocking at high reinforcement ratios. The mechanical properties also indicated that the addition of TiO_2 improved the mechanical properties, increased the hardness and decreased the sliding wear rate, especially following thermal sintering. The results of the thermal parameter tests showed that adding the reinforcement material reduced the conductivity and increased the thermal resistance. This demonstrates that it is possible to use oxides as reinforcement and for strengthening materials within the protective coatings of the turbine blades because they work as a heat insulator, with only a small portion of them not reaching the surface of the turbine blades.

References

[1] D. Dhand, P. Kumar and J.S. Grewal, "A review of thermal spray coatings for protection of steels from degradation in coal-fired power plants", *Corros. Rev.*, 39(3) (2021) 243-268.

[2] D. Qadir et al., "A review on coatings through thermal spraying", *Chem. Papers.*, 78(1) (2024) 71-91.

[3] R. Gao et al., "Material system and tribological mechanism of plasma sprayed wear resistant coatings: Overview", *Surf. Coat. Technol.*, 483 (2024) 130758.

[4] B. Swain, S.S. Mohapatra and A. Behera, "Plasma spray coating: a weapon to fight with erosion and corrosion phenomena", in: **Thermal Spray Coatings**, CRC Press (2021), pp. 317-330.

[5] T.S. Chowdhury et al., "A critical review on gas turbine cooling performance and failure analysis of turbine blades", *Int. J. Thermofluids*, 18 (2023) 100329.

[6] M.I. Boulos et al., "Plasma in the thermal spray coating industry", in: **Handbook of Thermal Plasmas**, Cham: Springer International Publishing (2023), pp. 1423-1508.

[7] M.A. Abdullah, R.Z. Hadi and S.Y. Darweesh, "Protection of turbine blades by adding metals to ceramic materials using flame coating method", *J. King Saud Univ. – Eng. Sci.*, (2024), doi: 10.1016/j.jksues.2024.02.001.

[8] M.N. Ahmed, N.A. Daham and S.Y. Darweesh, "Structural and mechanical properties for (Ni–WC) system by using thermal spray", *AIP Conf. Proceed.*, 2885(1) (2024) 181722.

[9] M.G. Kareem, A.M. Ali and S.Y. Darweesh, "Effect of adding yttria-stable zirconia to the compound (Al–Cr) on the hardness and porosity of the coating prepared by thermal spraying technique", *AIP Conf. Proceed.*, 2885(1) (2024) 181853.

[10] V. Lakkannavar et al., "A review on tribological and corrosion behaviour of thermal spray coatings", *J. Instit. Eng. (India): Ser. D*, (2024) 1-17, doi: 10.1007/s40033-024-00636-5.

[11] R.S. Antar, S. Darweesh and F.W. Ridha, "Production of a double cermet coating to treatment of the turbine blades", *Eng. Res. Exp.*, (2024), doi: 10.1088/2631-8695/ad2f82.

[12] P. Bharathi and T.S. Kumar, "Mechanical characteristics and wear behaviour of Al/SiC and Al/SiC/B4C hybrid metal matrix composites fabricated through powder metallurgy route", *Silicon*, 15(10) (2023) 4259-4275.

[13] Z.N. Majeed et al., "Improvement of aluminum properties by adding tungsten carbide using powder metallurgy", *Phys. Chem. Solid State*, 25(1) (2024) 203-211.

[14] J.C. Wang, H. Dommati and S.J. Hsieh, "Review of additive manufacturing methods for high-performance ceramic materials", *The Int. J. Adv. Manufact. Technol.*, 103 (2019) 2627-2647.

[15] S. Sattar et al., "Corrosion reduction in steam turbine blades using nano-composite coating", *J. King Saud Univ. – Sci.*, 35(8) (2023) 102861.
[16] K.L. Arun, M. Udhayakumar and N. Radhika, "A comprehensive review on various ceramic nanomaterial coatings over metallic substrates: applications, challenges and future trends", *J. Bio Tribo-Corros.*, 9(1) (2023) 11.
[17] S.A. Farooq et al., "Nanostructured coatings: review on processing techniques, corrosion behaviour and tribological performance", *Nanomaterials*, 12(8) (2022) 1323.
[18] S.Y. Darweesh, R.A. Rasheed and M.A. Abdullah, "Treatment of failures in turbine blades by cermet coatings", *J. Failure Anal. Prevent.*, 23(6) (2023) 2461-2470.
[19] H.H. Ahmed et al., "Processing of turbine blades using cermet composite materials", *J. Failure Anal. Prevent.*, 20 (2020) 2111-2118.
[20] E.J. Salih, S.M.A. Allah and S.Y. Darweesh, "Study the structural and mechanical properties of the Cu–WC composite", *AIP Conf. Proceed.*, 2398(1) (2022) 094030.
[21] P. Gkomoza et al., "Comparative study of structure and properties of thermal spray coatings using conventional and nanostructured hydroxyapatite powder, for applications in medical implants", *Surf. Coat. Technol.*, 357 (2019) 748-758.
[22] M.S. Baltatu et al., "Microstructural analysis and tribological behavior of Ti-based alloys with a ceramic layer using the thermal spray method", *Coatings*, 10(12) (2020) 1216.
[23] D. Chicot et al., "Hardness of thermal sprayed coatings: relevance of the scale of measurement", *Surf. Coat. Technol.*, 268 (2015) 173-179.
[24] A.S. Hajare and C.L. Gogte, "Comparative study of wear behaviour of thermal spray HVOF coating on 304 SS", *Mater. Today: Proceed.*, 5(2) (2018) 6924-6933.
[25] P. Fauchais, G. Montavon and G. Bertrand, "From powders to thermally sprayed coatings", *J. Therm. Spray Technol.*, 19 (2010) 56-80.
[26] D.Y. Darweesh and Z.N. Majid, "Improving the durability of streak and thermal insulation of petroleum pipes by using polymeric-based paint system: polymer matrix composites have several and wide applications", *Baghdad Sci. J.*, 17(3) (2020) 826.
[27] F.W. Ridha, "Calculation of thermal conductivity, mechanical properties values at adding copper to a base of zirconia by powder method", *Al-Bahir J. Eng. Pure Sci.*, 4(1) (2024) 3.
[28] A.M. Ibraheem, S.M.A. Allah and S.Y. Darweesh, "Enhancement the properties of aluminum by adding boron carbide by the powder method", *J. Phys.: Conf. Ser.*, 1999(1) (2021) 012074.
[29] R.M. Trommer and C.P. Bergmann, **Flame Spray Technology: Method for Production of Nanopowders**, Cham: Springer (2015).
[30] T.A. Owoseni, "Development of nanostructured ceramic coatings from suspension and solution precursor thermal spraying process", PhD dissert., University of Nottingham, UK (2021).
[31] N. Kumar and V.K. Choubey, "Recent trends in coating processes on various AISI steel substrates: a review", *J. Mater. Sci.*, 59(2) (2024) 395-422.
[32] B. Bülbül and M. Okumuş, "Microstructure, hardness, thermal and wear behaviours in Al–10Ni/TiO_2 composites fabricated by mechanical alloying", *Mater. Chem. Phys.*, 281 (2022) 125908.
[33] K.J. Joshua, S.J. Vijay and D.P. Selvaraj, "Effect of nano TiO_2 particles on microhardness and microstructural behavior of AA7068 metal matrix composites", *Ceram. Int.*, 44(17) (2018) 20774-20781.
[34] C.A.V. Kumar and J.S. Rajadurai, "Influence of rutile (TiO_2) content on wear and microhardness characteristics of aluminium-based hybrid composites synthesized by powder metallurgy", *Trans. Nonferrous Metals Soc. China.*, 26(1) (2016) 63-73.
[35] H. Dhiflaoui, K. Kaouther and A.B.C. Larbi, "Wear behavior and mechanical properties of TiO_2 coating deposited electrophoretically on 316L stainless steel", *J. Tribol.*, 140(3) (2018) 031603.
[36] J.A. Prakash et al., "Evaluation of mechanical, microstructural and tribological properties of ADC-12 composite reinforced with TiO_2 and WC", *AIP Conf. Proceed.*, 2861(1) (2023) 159876.
[37] M.E. Elmowafy et al., "Exploring a novel approach for the synthesis of MIL-53(Fe)/reduced graphene oxide composites with preserved structural integrity for high performance electromagnetic wave shielding", *Discover Appl. Sci.*, 6(4) (2024) 161.
[38] S.H. Humeedi, S.M. Abdulkareem and S.Y. Darweesh, "The synthetic and mechanical properties of a silica matrix cermet composite", *J. Wuhan Univ. Technol. – Mater. Sci. Ed.*, 37(3) (2022) 423-428.
[39] A.S. Karim, Z.N. Majeed and S.Y. Darweesh, "The effect of nanostructured zirconia reinforcement on the mechanical and structural properties of a copper-based system", *Mater. Sci. Forum*, 1039 (2021) 297-306.